



Contents lists available at ScienceDirect

## Journal of King Saud University – Science

journal homepage: [www.sciencedirect.com](http://www.sciencedirect.com)

## Original article

## Development, structural investigation, DNA binding, antimicrobial screening and anticancer activities of two novel quari-dentate VO(II) and Mn (II) mononuclear complexes

Laila H. Abdel-Rahman<sup>b</sup>, Ahmed M. Abu-Dief<sup>a,b,\*</sup>, Azza A. Hassan Abdel-Mawgoud<sup>b</sup><sup>a</sup>Departamento de Quimica Organica e Inorganica, Facultad de Quimica, Universidad de Oviedo, 33006 Oviedo, Spain<sup>b</sup>Chemistry Department, Faculty of Science, Sohag University, 82524 Sohag, Egypt

## ARTICLE INFO

## Article history:

Received 29 March 2017

Accepted 11 May 2017

Available online 17 May 2017

## Keywords:

Imines

Structural elucidation

Antimicrobial screening

DNA binding

Anticancer efficiency

## ABSTRACT

Two novel VO(II) and Mn(II) imine chelates derived from the condensation of o-phenylenediamine (PN) with 3-ethoxysalicylaldehyde(ES) were synthesized. The prepared ESPN imine ligand and its chelates were investigated *via* different analytical and physicochemical tools. Correlation between all the obtained results, the parent ligand behaves as tetra-dentate ONNO ligand and coordinates to Mn(II) and VO(II), in octahedral and square pyramidal geometry, respectively. Also, the prepared compounds were screened for their antimicrobial activities on different pathogenic bacteria and fungi. The results show that the complexes have a stronger antimicrobial activity in comparison with its ligand. Moreover, the interaction of the prepared metal chelates with CT-DNA was detected utilizing spectral studies, viscosity and gel electrophoresis measurements. The obtained results clearly demonstrate that, the binding affinity with CT-DNA for ESPN > ESPNV complex. Furthermore, the cytotoxic activity of the tested compounds on human colon carcinoma cells, hepatic cellular carcinoma cells and breast carcinoma cells has been examined. From these results it was found that the investigated complexes have effective cytotoxicity against growth of carcinoma cells with respect of its imine ligand.

© 2017 The Authors. Production and hosting by Elsevier B.V. on behalf of King Saud University. This is an open access article under the CC BY-NC-ND license (<http://creativecommons.org/licenses/by-nc-nd/4.0/>).

## 1. Introduction

Imine ligands are deemed privileged ligands, because most of them are easily prepared by a simple one-pot condensation of aldehydes and primary amines in an alcohol solvent. Their ease of synthesis, multi denticity, forming stable complexes usually through the imine nitrogen and other atoms like oxygen, sulfur or nitrogen with vital applications in catalysis, molecular biology, molecular ferromagnets design, liquid crystals (Canali and Sherrington, 1999; Lin et al., 2003; Abu-Dief et al., 2015), medical imaging (Tisato et al., 1994) and optical materials (Lacroix 2001). Moreover, imine ligands are able to coordinate many different

metals (Abu-Dief et al., 2013; Gupta et al., 2009; Gupta and Sutar, 2007; Ligtenberg et al., 2003; Abu-Dief and Mohamed, 2015), and to stabilize them in various oxidation states. Furthermore, imine metal chelates have been utilized as drugs and they have a broad variety of antimicrobial efficiency against bacteria, fungi, and specific type of tumors (Abdel-Rahman et al., 2014; Abdel-Rahman et al., 2015a; Abdel-Rahman et al., 2016a,b,c; Abdel-Rahman et al., 2017a–d). Drugs activity is increased when treated as metal chelates and block the expansion of tumors (Datta et al., 2002). Manganese(II) chelates have structural support for proteins as arginase, pyruvate carboxylase and ribonuclease hydrolases concanavalin. Moreover, Mn(II) plays an vital role in the metabolism of biological systems such as manganese peroxidase, superoxide dismutase and manganese(II) dioxygenase (Maneiro et al., 2001).

On the other hand, the interest in vanadium coordination chemistry advocated by its presence in biological systems, and by catalytic (Rayati et al., 2010), and medicinal (Keypour et al., 2008) properties of its compounds. The potency catalytic abilities of vanadium compounds give the great interest of vanadium coordination chemistry in modern years (Ligtenberg et al., 2003). Thus, in the current study, we record synthesis of VO(II) and Mn (II)

\* Corresponding author at: Chemistry Department, Faculty of Science, Sohag University, 82524 Sohag, Egypt.

E-mail address: [ahmed\\_benzoic@yahoo.com](mailto:ahmed_benzoic@yahoo.com) (A.M. Abu-Dief).

Peer review under responsibility of King Saud University.



Production and hosting by Elsevier

incorporating tetra-dentate ESPN imine ligand. The structure of the prepared compounds was checked different spectroscopic techniques. In addition to, the biological efficiency of the parent ligand and its metal chelates was maintained against selected kinds of bacteria and fungi. Moreover, binding of the prepared imine chelates with CT-DNA was studied. Furthermore, anti-cancer activity of the prepared compounds were tested.

## 2. Experimental

### 2.1. Reagents

The solvents and reagents used for our study were of commercially available reagent degree and used wanting purification. They contain 3-ethoxysalicylaldehyde, *o*-phenylenediamine, vanadyl acetylacetonate ( $\text{VO}(\text{C}_5\text{H}_7\text{O}_2)_2$ ), manganese chloride ( $\text{MnCl}_2$ ) Calf thymus DNA(CT-DNA), Tris[hydroxymethyl]-aminomethane (Tris), bromophenol blue dye and ethidium bromide were obtained from Merck.

### 2.2. Preparation of ESPN imine ligand

The tetra-dentate ESPN imine ligand (cf. Scheme 1) was synthesized by the condensation of 3-ethoxysalicylaldehyde (10 mmol 1.66 g) with *o*-phenylenediamine (5 mmol, 0.54 g) in ethanol. The obtained reaction mixture was refluxed for 1 h at 80 °C in presence of few drops of piperidine as catalyst. After that, solutions were gradually evaporated to half of its original volume and then left to cool. The completion of the reaction mixture was monitored by TLC. The obtained orange crystals of ESPN imine ligands were filtered. Then washed various times with cold ethanol and exsiccated in a desiccator (Majumder et al., 2009; Nejo et al., 2011).

$^1\text{H}$ NMR ( $\delta$ , ppm), in DMSO:  $\delta$  = 1.38 (s, 6H,  $\text{CH}_3$ ), 4.12 (d,  $^3J = \text{Hz}$ , 4H,  $\text{CH}_2$ ), 6.92 (t,  $^3J = 8.0 \text{ Hz}$ , 2H, H-5,5'), 7.08 (d,  $^3J = 4.1 \text{ Hz}$ , 2H, H-4,4'), 7.29 (s, 2H, H-6,6'), 7.64 (d,  $^3J = 7.9 \text{ Hz}$ , 4H, H-8,9,10, 11), 7.71 (s, 2H, CH = N), 13.08 ppm (s, 2H, –OH). (cf. Fig. S1).

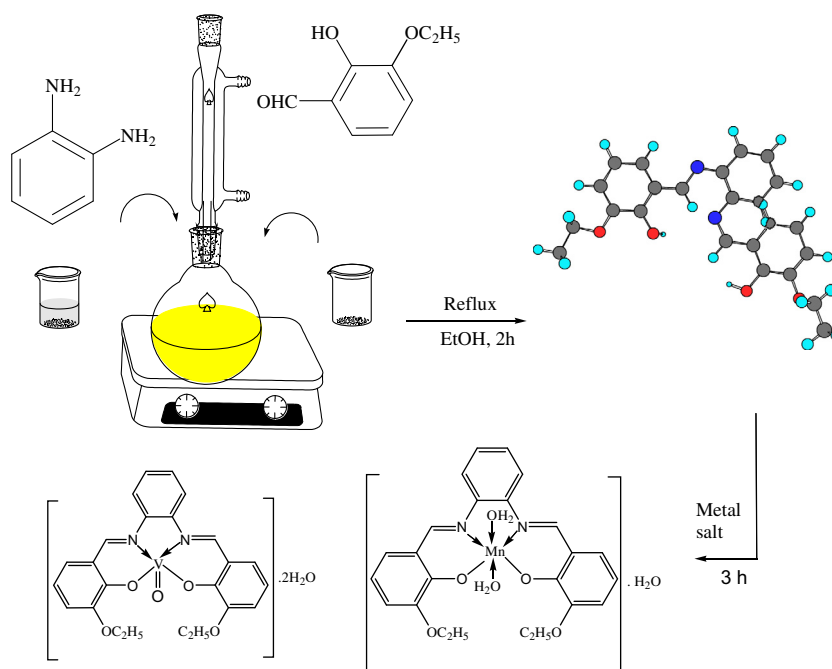
$^{13}\text{C}$ NMR ( $\delta$ , ppm), in DMSO:  $\delta$  = 15.2 (CH,  $\text{CH}_3$ ), 64.7 (CH,  $\text{CH}_2$ ), 116.4 (CH), 118.4 (CH), 119.0 (CH), 123.2 ( $\text{C}_q$ ), 128.1 ( $\text{C}_q$ ), 133.6 ( $\text{C}_q$ ), 141.3 ( $\text{C}_q$ ), 148.2 (CH), 149.3 (CH), 152.4 ppm (CH = N). (cf. Fig. S2).

### 2.3. Preparation of ESPNMn and ESPNV imine complexes

The titled imine VO(II) and Mn(II) complexes were obtained according to a general procedure: 10 mmole (4.05 g) of ESPN ligand was dissolved in ethanol and 10 mmole of metal salt (1.98 g of Mn (II) or 2.65 VO(II)) was dissolved in aqueous-ethanolic mixture. The two solutions were mixed together and refluxed for 2 h at 85 °C. After evaporation the solvent, the precipitated solid was filtered off from the reaction mixture, thoroughly washed thoroughly with EtOH to remove any traces of un-reacted starting materials, and dried under vacuum. The purity of the chelates was investigated by TLC (cf. Scheme 1).

### 2.4. Characterization of the tested ESPN imine ligand and its complexes

Melting point for the prepared imine ligand and degradation temperatures for its tested metal chelates were performed on a melting point device, Gallenkamp, UK. Infrared spectra were recorded as KBr pellets using Shimadzu FTIR-8300 spectrophotometer.  $^1\text{H}$  and  $^{13}\text{C}$  NMR spectra were obtained in deuterated DMSO solutions with a Bruker Avance DPX-500 spectrometer. UV–Vis spectra of the prepared compounds in DMF were recorded utilizing 10 mm matched quartz cells via PG spectrophotometer model T + 80. Micro analytical data were carried out using Elemental analyzer Perkin-Elmer (model240c). The instrument employed for recording magnetic susceptibility is Gouy's balance. Molar conductivity measurements were performed using JENWAY 4510 conductivity meter. TGA was done on Shimadzu corporation 60H analyzer with a heating rate  $10 \text{ }^\circ\text{C min}^{-1}$  under nitrogen. An ADWA AD1000 and AD1020 pH meter was utilized to pH measurements and standardized using criterion buffers (pH 4.02 and 9.18) previously mensuration.



**Scheme 1.** Synthetic strategy for the preparation of the investigated complexes.

## 2.5. Evaluation of the stoichiometry of the prepared imine metal chelates

The molar ratio (Abdel-Rahman et al., 2015a,b; Abdel-Rahman et al., 2016a,b) and continuous variation methods were employed to determination metal to ligand ratio (Abdel-Rahman et al., 2014; Abdel-Rahman et al., 2016 a,b; Abu-Dief and Nassr, 2015).

### 2.5.1. Estimation of the stability and formation constants of the prepared imine metal chelates

The formation constants ( $K_f$ ) of the studied imine chelates in solutions were obtained by employing spectrophotometric measurements using the continuous variation method (Abdel-Rahman et al., 2014; Abdel-Rahman et al., 2016a,b; Abu-Dief and Nassr, 2015) according to the following relation:

$$K_f = \frac{A/A_m}{(1 - A/A_m)^2 C} \quad (1)$$

where  $A_m$  is the absorbance at the maximum formation of the complex,  $A$  is arbitrarily selected absorbance values on either side of the absorbance peak and  $C$  is the initial molar concentration of the metal. Also, the free energy change,  $\Delta(G^*)$  of the complexes was determined by  $\Delta(G^*) = -RT \ln K_f$ , at 25 °C.

## 2.6. Kinetic studies

The kinetic parameters of decomposition process for metal complexes were extracted from Coast-Redfern integral method (Abdel-Rahman et al., 2015a,b). Thermodynamic parameters such activation energy ( $E^*$ ), activation entropy ( $\Delta S^*$ ), enthalpy ( $\Delta H^*$ ) and free energy change ( $\Delta G^*$ ) of the decomposition of the metal complexes were estimated by employing the following equation,

$$\log \left[ \frac{\log(w_{\infty}/(w_{\infty} - w))}{T^2} \right] = \log \left[ \frac{AR}{\phi E^*} \left( 1 - \frac{2RT}{E^*} \right) \right] - \frac{E^*}{2.303RT} \quad (2)$$

where  $w$  is the mass loss at temperature certain  $T$ ,  $w_{\infty}$  is the mass loss of completion of the decomposition reaction,  $R$  is the universal gas constant and  $\phi$  is the heating rate. A plot of the left-hand side of Eq. (1) against reciprocal of  $T$  gives a slope from which  $E^*$  was calculated and  $A$  was determined from the intercept. The other thermo-kinetic parameters were calculated utilizing the following equations (Abdel-Rahman et al., 2016a,b,c):

$$\Delta S^* = 2.303R \log \frac{Ah}{K_B T} \quad (3)$$

$$\Delta H^* = E^* - RT \quad (4)$$

$$\Delta G^* = H^* - T\Delta S^* \quad (5)$$

where  $(h)$  and  $(K_B)$  are Boltzmann's and Plank's constants, respectively.

## 2.7. Antimicrobial activities of the prepared compounds

The biological activities of the presented ESPN imine ligand and its chelates were tested against various species of bacteria (*Escherichiacoli* (-ve), *Bacillussubtilis* (+ve) and *Staphylococcus aureus* (+ve)) via well diffusion method (Abdel-Rahman et al., 2013; Abdel-Rahman et al., 2014; Abdel-Rahman et al., 2015a,b; Abdel-Rahman et al., 2016a,b,c; Abu-Dief and Nassr, 2015). The antifungal effect of the complexes were also tested by utilizing the well diffusion method against various species of fungi (*Aspergillus niger*, *Candida glabrata* and *Trichophyton rubrum*) on potato dextrose agar as environment. Molar concentrations 10 and 20 (mg/ml) of the investigated compounds have prepared in

dimethylsulfoxide. The well was filled with the prepared solution using a micropipette and the plate was improved 24 h at 37 °C for the bacteria or 72 h at 35 °C for the fungi. After incubation, the diameter of the obtained zone of inhibition around the sample was taken as a criterion of the inhibitory power of the compound against investigated microbe with zone reader (Hi Antibiotic zone scale). The standard antibacterial drug, Gentamycin and anti-fungi drug, Fluconazole were also screened under similar conditions for comparison. DMSO was used as blank solvent for antimicrobial activity due to its negligible effect on the bacteria and fungi.

## 2.8. DNA-interaction propensity

Each of the tests including the interaction of the chelates with CT-DNA were performed in Tris–HCl buffer (60 mM, pH7.2). CT-DNA was purified by centrifugal dialysis previously utilize. A solution of calf thymus DNA in the buffer gave a ratio of UV absorption at 260 and 280 nm of about > 1.85, suggesting that the DNA was appropriately liberated of protein profanation (Abdel-Rahman et al., 2016a,b,c; Abdel-Rahman et al., 2017a–e). The concentration of DNA per nucleotide was evaluated via oversight the UV absorbance at 260 nm utilizing  $\epsilon_{260} = 6600 \text{ mol}^{-1} \text{ cm}^2$ . parent solution was retained at 4 °C and utilized only through one day.

### 2.8.1. Electronic spectra for the interaction of complexes with DNA

Spectrophotometric scan test was carried out by conservation of the molar concentration of complex constant while changing [DNA] in the surrounding conditions. The absorption of free CT-DNA was removed using clear buffer solution in the blank compartment (Abdel-Rahman et al., 2016a,b,c). From the absorption information, the actual binding constant ( $K_b$ ) was limited using plotting [CT-DNA]/( $\epsilon_a - \epsilon_f$ ) vs. [DNA] utilizing the following equation:

$$\frac{[DNA]}{(\epsilon_a - \epsilon_f)} = \frac{[DNA]}{(\epsilon_b - \epsilon_f)} + \frac{1}{[K_b(\epsilon_b - \epsilon_f)]} \quad (6)$$

where, [CT-DNA] is the molar concentration of DNA in base pairs,  $\epsilon_a$ ,  $\epsilon_f$  and  $\epsilon_b$  are the obvious, free and fully bound complex extinction coefficients, respectively. The standard Gibb's free energy for DNA binding was evaluated from the following relation (Abdel-Rahman et al., 2013; Abdel-Rahman et al., 2015a,b)

$$\Delta G_b^{\ddagger} = -RT \ln K_b \quad (7)$$

### 2.8.2. Hydrodynamic measurements

Hydrodynamic measurements were executed utilizing an Oswald micro viscometer, kept at constant temperature (298 K). The fluidity times were registered to different molar concentrations of the complex (5–50  $\mu\text{M}$ ), maintenance the concentration of DNA steady (260  $\mu\text{M}$ ). Combination of the solution was obtained by bubbling the nitrogen gas via the viscometer. The buffer fluidity time in seconds was registered as  $t^{\circ}$ . The relative viscosities for CT-DNA in the presence ( $\eta$ ) and absence ( $\eta^{\circ}$ ) of the sample were determined hiring the relation  $\eta = (t - t^{\circ})/t^{\circ}$ . Where,  $t$  is the observed time of fluidity in seconds and the magnitudes of the relative viscosity ( $\eta/\eta^{\circ}$ ) were figured against  $1/R$  ( $R = [\text{DNA}]/[\text{Complex}]$ ) (Abdel-Rahman et al., 2013; Abdel-Rahman et al., 2016a,b,c; Abdel-Rahman et al., 2017a–e).

### 2.8.3. DNA interaction using agarose gel electrophoresis

DNA-complex adducts were investigated using agarose gel electrophoresis photograph. The parent buffer solution of compounds was destined by dissolving 20 mg of the prepared complexes in 20 ml of DMF. The sample (25  $\mu\text{g}/\text{ml}$ ) was added up to the buffered solution of DNA and incubated for 1 h at  $37 \pm 1$  °C and then 30  $\mu\text{l}$  of

DNA sample (mixed with bromophenol blue dye at a 1:1 ratio) was carried by noting to the electrophoresis chamber wells along with a standard DNA tick in TBE buffer and then loaded onto the agarose gel, then an invariable electricity (60 V) was utilized to about 40 min. Finally, the gel was separated and spotted with 20 µg/ml of ethidium bromide for 15–20 min. The bands acquired was spotted under UV light utilizing a transilluminator accompanied by photography with DMC-LZ5 Lumix Digital Camera to mark the range of DNA binding contrasted with the buffer solution of DNA tick (Abdel-Rahman et al., 2016a,b,c; Abdel-Rahman et al., 2017a–e; Abu-Dief and Nassr, 2015).

### 2.9. Cytotoxic activity of the investigated compounds

Cytotoxic activity was performed at Faculty of Pharmacy, Pharmacology Department, Assuit University. Optical density (O.D.) of every well was measured spectrophotometrically at 564 nm) with an “ELIZA” micro plate reader. Estimation of anti-cancer activities of the prepared ESPN imine ligand and its metal chelates was executed versus human Colon carcinoma cells (HCT-116 cell line), hepatic cellular carcinoma cells (HepG-2) and breast carcinoma cells (MCF-7 cell line). The estimation experiment was executed *in vitro* utilizing the Sulfo-Rhodamine-B-stain (SRB) (Abu-Dief et al., 2016; Hindo et al., 2009). The investigated cells were put in 96-multiwell plate ( $10^4$  cells/well) for 24 hrs before souring to the samples to permit correlation of cell to the wall of the plate. Different molar concentrations of the samples beneath investigation through dimethylsulfoxide (0, 1, 2.5, 5 and 10 µM) were gathered to the monolayer of the cell. These cells were brood together with the prepared compounds for 48 hrs at 37 °C and in 5% CO<sub>2</sub> atmosphere. After 48 h, cells were firmed, swilled, and spotted with Sulfo-Rhodamine-B-stain. Speck surplus was lotion with acetic acid and linked stain was handled with Tris EDTA buffer. IC<sub>50</sub> was estimated and reactivity was determined with respect to change percentage of (vistabline as reference drug) (Abdel-Rahman et al., 2016c; Abu-Dief et al., 2016) following to the equation:

$$(IC)\% = (\text{Control O.D.} - \text{Sample O.D.}) \times 100 / \text{Control O.D.} \quad (8)$$

## 3. Results and discussion

### 3.1. Structure elucidation of prepared ESPN imine ligand and its complexes

#### 3.1.1. NMR spectra of the prepared ESPN imine ligand

The formation of the prepared ESPN imine ligand was further supported by the NMR spectral study. The <sup>1</sup>H and <sup>13</sup>CNMR spectral data of the prepared ligand are recorded in the experimental section (cf. Figs. S1 and S2). The <sup>1</sup>HNMR spectrum of ESPN imine ligand showed two singlet signals at δ = 13.08 ppm, that are assigned to the two phenolic –OH. Also, it shows singlet signal at δ = 7.71 which is characteristic for azomethine (CH = N) proton of the ligand (Mounika et al., 2011; Alaghaz et al., 2015; Abdel-Rahman et al., 2016a–d). Moreover, it shows multiplet signals at 7.64–6.92 ppm for aromatic of 10- CH protons. <sup>13</sup>C NMR of ESPN imine ligand exhibited signal at 152.4 ppm may be assigned to azomethine carbon. The signals observed in the region 149.3– 116.4 ppm were assigned to phenyl carbons. While signals observed in the region 64.7 due to –CH<sub>2</sub>- group and 15.2 due to –CH<sub>3</sub> group

#### 3.1.2. Elemental analysis and electrical conductivity measurements

The elemental analysis results of the prepared imine ligand and its complexes are recorded in Table 1 and suggested that ESPN

imine ligand act as tetra-dentate and form complexes with VO(II) and Mn(II) in 1: 1 rate metal to ligand (cf. Scheme 2). The molar conductance of the tested metal chelates was observed at room temperature in DMF as a solvent and their results are recorded in Table 1. The molar conductance values of all prepared complexes fall into the range (3.15–4.50) Ω<sup>-1</sup> cm<sup>2</sup> mol<sup>-1</sup>) assigned to their non- electrolytic behaviour (Rapheal et al., 2007; Chandra et al., 2008; Abdel-Rahman et al., 2013; Abdel-Rahman et al., 2016a–d)

#### 3.1.3. Infrared spectra

The bonding of the prepared ESPN imine ligand to the metal ions has been judged by a careful comparison of the infrared spectra of the metal complexes with those of the free ligand. The characteristic IR frequencies of the ESPN ligand and its metal chelates along with their assignments (cf. Table S1 and Figs. S3–S4). Bands because of –OH and –CH=N are distinguishable and offer proof considering the structure of the ligand and its bonding with metal. A band at 1622 cm<sup>-1</sup> in the ESPN ligand is due to –C=N stretching vibration. On complexation, this band is displaced to a lower frequency (1600–1602 cm<sup>-1</sup>). The negative shift of this band is an obvious significance of the involvement of the azomethine nitrogen atoms in metal chelate formation (Begum et al., 2010; Abdel-Rahman et al., 2014; Abdel-Rahman et al., 2016a,b,c,d). This is confirmed by the existence of band at 436 and 463 cm<sup>-1</sup> corresponding to the stretching vibration of M–N bond in ESPNMn and ESPNV, respectively. Bands at 561–564 cm<sup>-1</sup> correspond to M–O stretching vibrations. Band at 3478 cm<sup>-1</sup> observed in the ligand spectrum is because of stretching vibrations of free –OH. In the metal chelates, the recorded IR spectra of all the tested imine compounds indicate broad band at 3419, 3418 cm<sup>-1</sup> which have been referred to ν(OH) stretching vibration of crystalized water molecules, in accordance with the returns of the elemental analysis recorded in (Table 1). In the low wave number region, ESPN imine ligand indicated an absorption band at 1230 cm<sup>-1</sup> which can outcome from the expansibility vibration of the phenolic (C–O) group. The shifting of that band to lower wave number values onto coordination suggested that the oxygen atoms of the phenolic groups are consistent to the metal ion. moreover, IR spectra of (VO) complexes at 943–988 cm<sup>-1</sup> which is referred to vibration of VO(II) in monomeric complexes as reported in previous publications (Rayati et al., 2010; Nejo et al., 2011).

#### 3.1.4. Electronic spectra

The electronic absorption spectra of ligand and its metal chelates were recorded at the wavelength extent 800–200 nm and room temperature (cf. Table S2 and Fig. 1, S5). The ligand presents absorption bands in UV–Vis region at 349 nm which is referred to n → π\* transition resulting from the imine assignment of the imine ligand (Silverstein and Webster, 1997). The absorption bands of complexes at λ<sub>max</sub> = 310, 324 nm is assigned to charge transfer with in ESPN imine ligand to VO (II) and Mn(II). Furthermore, an extended and a broad band which is existed in the zone 527, 421 nm for ESPNMn and ESPNV complexes, respectively. This band could assigned to the d → d transition in the structure of the tested metal chelates (cf. Table S1) (Dyer, 1965).

#### 3.1.5. Magnetic moment measurements

The observed magnetic moment for complexes are generally diagnostic of the coordination geometry about the metal ion (cf. Table 1). Magnetic susceptibility measurements (cf. Table 1) suggested that the tested ESPNMn complex has paramagnetic character showed high spin magnitude (5.32 B.M.) i.e., the studied ESPN imine ligand is so weak that it exhibited low t<sub>2g</sub> and e<sub>g</sub> d- splitting of the octahedral structures of the complexes (Raman et al., 2002; Canpolat and Kaya, 2002; El-Tabl et al., 2008; Abdel-Rahman et al., 2015a,b). The magnetic susceptibility of ESPNV complex has a



**Table 1**  
Micro analytical and physical data of the prepared ESPN ligand and itschelates.

Compounds [Molecular formula]	M.wt	Color	Yield (%)	$\Lambda_m$ ( $\Omega^{-1} \text{ cm}^2 \text{ mol}^{-1}$ )	$\mu_{\text{eff}}$ (B.M.)	M.p and Dec. temp ( $^{\circ}\text{C}$ )	Analysis (%) Found (calcd.)			
							C	H	N	M
ESPN $\text{C}_{24}\text{H}_{24}\text{N}_2\text{O}_4$	404.17	Brown	(84)	–	–	195	71.34 (71.27)	5.91 (5.98)	6.87 (6.93)	
ESPNMn $\text{C}_{24}\text{H}_{28}\text{MnN}_2\text{O}_7$	510.94	Black	(83)	3.15	5.32	(280)	56.43 (56.37)	5.42 (5.48)	5.54 (5.48)	10.64 (10.75)
ESPNVC $\text{C}_{24}\text{H}_{26}\text{N}_2\text{O}_7\text{V}$	504.94	Green	(85)	4.50	1.75	(>300)	57.13 (57.04)	5.19 (5.15)	5.47 (5.55)	13.18 (13.26)

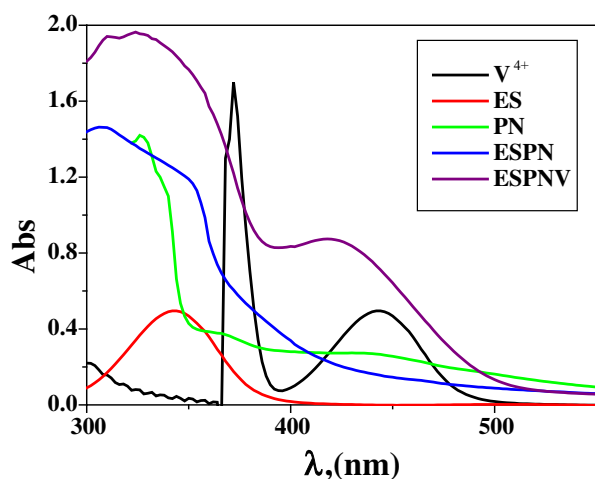


**Fig. 1.** Molecular electronic spectra of ESPNV complex and its components in DMF at 298 K.

magnetic moment value of 1.78 B.M., which is close to the spin-only value for  $d^1$  and in agreement with the reported values for square pyramidal complexes of VO(II) (Raman et al., 2002).

### 3.1.6. Thermal analysis

TGA of ESPNV complex (cf. Table 2 and Fig. S6) showed four stages of decomposition within the temperature range 30–850  $^{\circ}\text{C}$ . The first stage at 30–120  $^{\circ}\text{C}$  corresponds to the loss of two water molecules of hydration with mass loss of 7.05% (Calc. 7.13%). The second step 122–216  $^{\circ}\text{C}$  is related to elimination of a part of imine ligand ( $\text{C}_8\text{H}_8\text{O}_2$ ) with mass loss (Found 26.97% (calc. 26.94%) within the temperature range 223–481  $^{\circ}\text{C}$ . The third step 218–422  $^{\circ}\text{C}$  is related to elimination of another part of imine ligand ( $\text{C}_8\text{H}_8\text{O}_2$ ) with mass loss (Found 27.01% (calc. 26.94%). The terminal stage, in the temperature range 424–801  $^{\circ}\text{C}$ , is observed with mass loss of (Found 25.73%, Calc. 25.77%) corresponding to the elimination of organic residual ( $\text{C}_8\text{H}_6\text{N}_2$ ), resulting VO as residue.

**Table 2**  
Thermal degradation steps, mass losses (%), suggested lost fragments, final residue and thermo-kinetic parameters of each degradation step for the prepared complexes.

Complex	Dec. Temp. ( $^{\circ}\text{C}$ )	Mass loss (%)		Suggested segment	$E^{\ddagger}$ ( $\text{KJmol}^{-1}$ )	A ( $\text{S}^{-1}$ )	$\Delta H^{\ddagger}$ ( $\text{KJmol}^{-1}$ )	$\Delta G^{\ddagger}$ ( $\text{KJmol}^{-1}$ )	$\Delta S^{\ddagger}$ ( $\text{Jmol}^{-1} \text{ K}^{-1}$ )
		Found	(Calc.)						
ESPNV	30–120	7.05	(7.13)	$2\text{H}_2\text{O}$	255	0.24	253.8	287.5	–250.2
	122–216	26.97	(26.94)	$\text{C}_8\text{H}_8\text{O}_2$			253.6	294.6	–251.8
	218–422	26.99	(26.94)	$\text{C}_8\text{H}_8\text{O}_2$			252	337	–257.7
	424–801	25.73	25.75	$\text{C}_8\text{H}_6\text{N}_2$			249.8	412	–262.9
Residue	>801	13.29	(13.26)	VO	–	–	–	–	
ESPNMn	35–122	3.48	(3.52)	$\text{H}_2\text{O}$	61.0	0.062	59.5	79	–256.7
	124–215	7.09	(7.05)	$2\text{H}_2\text{O}$			58.2	119.6	–265.95
	217–513	32.01	(31.90)	$\text{C}_9\text{H}_9\text{NO}_2$			57	156.6	–269.85
	515–797	46.69	(46.78)	$\text{C}_{15}\text{H}_{13}\text{NO}_2$			54.7	234	–274.61
Residue	>797	10.71	(10.75)	Mn	–	–	–	–	

The thermogram of ESPNMn complex exhibited four decomposition steps within the temperature range 35–797  $^{\circ}\text{C}$ . The first step correspond to elimination of lattice water molecule with mass loss of (Found 3.48%, Calc. 3.52%). The second step of decomposition within the temperature range 124–215  $^{\circ}\text{C}$  corresponds to the loss of two coordinated water molecule, with a mass loss of 7.09% (Calc. 7.05%). The third and fourth steps are consistent with elimination of organic matter ( $\text{C}_9\text{H}_9\text{NO}_2$ ,  $\text{C}_{15}\text{H}_{13}\text{NO}_2$ ) with mass losses (Found 32.01, Calc. 31.90%) and (Found 46.69, Calc. 46.78%) within the temperature ranges 217–513  $^{\circ}\text{C}$  and 515–797  $^{\circ}\text{C}$  leaving Mn as a metallic residue (Shakir et al., 2016; Abdel-Rahman et al., 2016a–d).

**3.1.6.1. Kinetic aspects.** The thermo-kinetic parameters are found in Table 2. It is indicated that  $G^{\ddagger}$  magnitudes increase because of increase temperature. The positive magnitudes of  $H^{\ddagger}$  indicate that decomposition operations are endothermic. In all thermal steps,  $S^{\ddagger}$  is a negative value show that the degradation through unusual pathway and the decomposition processes are undesirable. The negative entropy of activation values give evidence for a more ordered activated state (Yousef et al., 2012).

### 3.1.7. Spectrophotometric determination of the stoichiometry of the tested complexes

Based on obtained results, the stoichiometry of the tested metal chelates is 1:1. The curves of the continuous variation method (cf. Fig. 2) offered maximum absorbance at mole fraction  $X_{\text{ligand}} = 0.5$ –0.6 suggesting the complexation of metal ions to ligand in molar ratio 1:1. Moreover, the data which consequence from using the molar ratio method subscribe the same metal ion to ligand ratio of the tested metal chelates (cf. Fig. S7) (El-Shiekh et al., 2011; Abdel-Rahman et al., 2015a,b)

**3.1.7.1. Estimation of the formation constants of the investigated imine chelates.** The formation constants ( $K_f$ ) of the investigated imine chelates were determined using the continuous variation method (cf. Table S3). As pointed in (Table S2), the acquired  $K_f$  magnitudes suggest the high stability of the prepared imine chelates. Negative magnitudes of Gibbs free energy show that the complexation

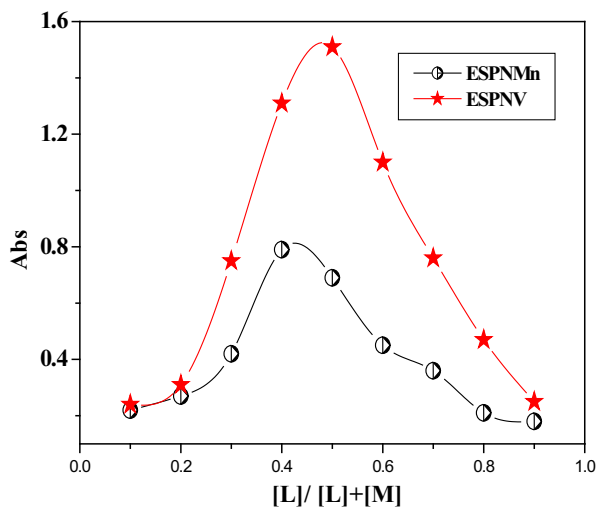


**Fig. 2.** Job's plots for determining the stoichiometry of the investigated imine chelates in aqueous – ethanolic medium at  $[ESPNV] = [ESPMn] = 10^{-3}$  M and 298 K.

process is spontaneous and favored. The pH-profile explained in (cf. Fig. 3) suggested idealistic dissociation detours and a height persistence pH range (4–10) of the prepared metal chelates. This indicates that the complex formalization highly settle down ESPN imine ligand. thus, the desired pH range for the various biological and industrial implementation of the investigated chelates is from pH = 4 to pH = 10. Fig. 6.

### 3.2. Antimicrobial activity Evaluation

All of the prepared complexes displayed good biological activity with the micro-organism (cf. Table S4 and Figs. 4 and 5). On contrasting the biological wares of the imine ligand, its complexes with those of a standard bactericide and fungicide, it was obvious that the metal chelates had conservative activity because of corresponded with the standard, but all the metal chelates were more active than free ligand. The highly inhibition zone of complexes of the transition metal than those of the ligand could be shown based on the Overtone notion and the complexation theory. when complexation occur, the polarity of the metal ion is decreased to a great range because of the interfere of the ligand orbital and the fragmentary sharing of the positive charge of the metal ion with donor groups (Al-Mogren et al., 2013; Abdel-Rahman et al.,

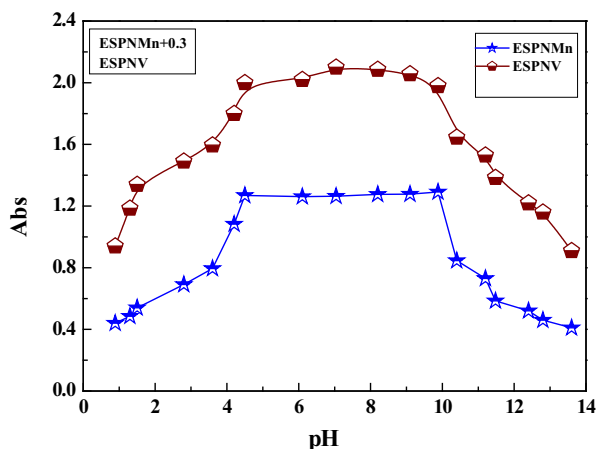


**Fig. 3.** Dissociation curve of the prepared imine complexes in DMF.

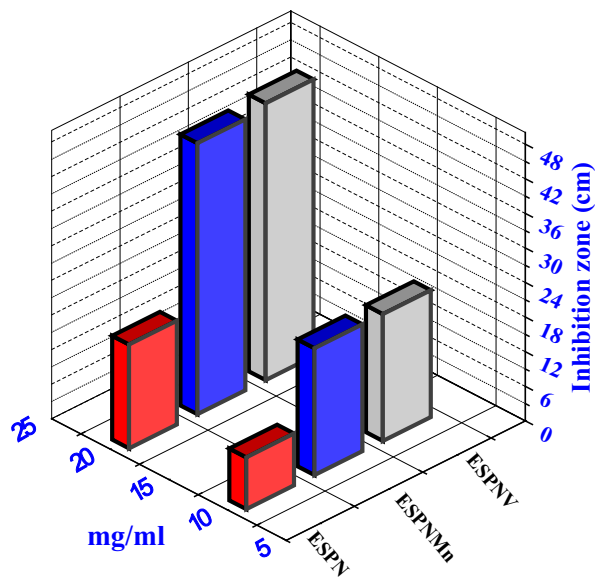


**Fig. 4.** Histogram indicating the comparative antibacterial activities of the prepared compounds versus *B. subtilis* bacteria.

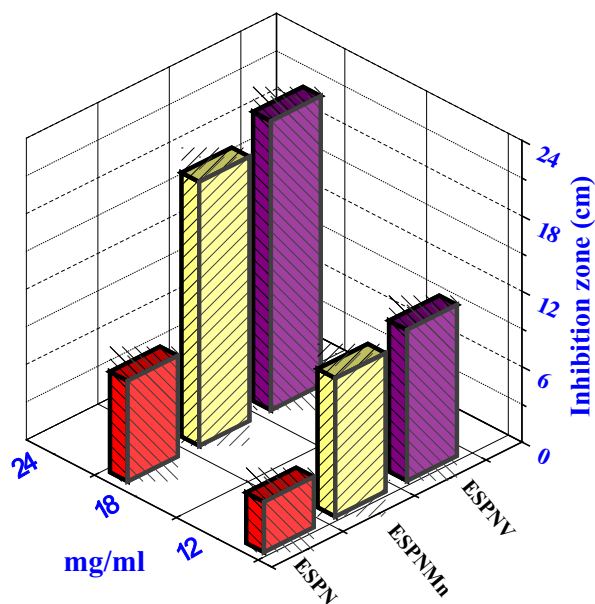


**Fig. 5.** Histogram indicating the comparative antifungal activities of the investigated compounds versus *T. rubrum* fungi.

2016a,b,c,d; Abu-Dief et al., 2016). The minimum inhibitory concentration (MIC) was evaluated by serial dilution method and shown in (Table 3). The ESPNV complex (3 mg/mL) was found to be highly effective as they exhibit the lowest MIC against *B. subtilis* bacteria and *Aspergillus flavus* fungi compared to ESPMn complex. The antimicrobial studies suggested that all the complexes exhibited safely promoted antimicrobial activity against microbial strains in comparison to the free ligands. The activities of the tested complexes were affirmed by estimation the potency index (Table S5) according to the following relationship (Abdel-Rahman et al., 2015a,b; Abdel-Rahman et al., 2017a–d)

$$\text{Activity index (A)} = \frac{\text{inhibition zone of complex (mm)}}{\text{inhibition zone of standard drug (mm)}} \times 100 \quad (9)$$

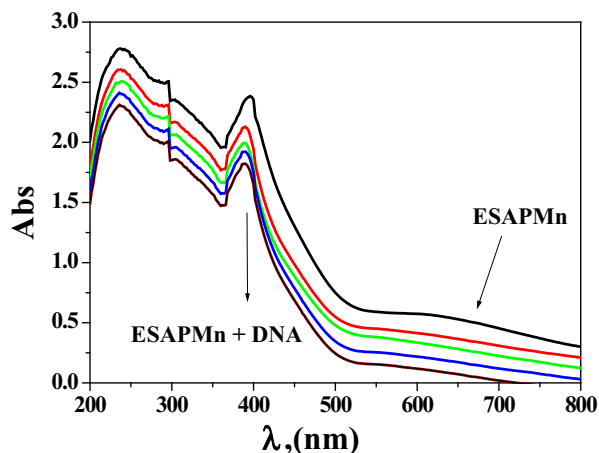


Fig. 6. Spectral scans of the interaction of ESPNMn complex ( $10^{-3}$  mol  $\text{dm}^{-3}$ ) in  $0.01$  mol  $\text{dm}^{-3}$  Tris buffer with CT-DNA ( $0$ – $30$ )  $\mu\text{M}$  DNA.

### 3.3. DNA binding potency

#### 3.3.1. Electronic spectra of interaction with DNA

The technique of electronic absorption spectroscopy is an active method for check the binding mode of DNA through chelates. The spectra were registered as a function of the addition of the buffer solutions of pure CT-DNA to the buffer solutions of the tested chelates. If the interaction mode is intercalation, the orbital of the inserted ligand can couple with the orbital of the base pairs, lowering the  $\pi$ – $\pi^*$  transition energy and lead to bathochromism. If the conjunction orbital is partially filled by electrons, it leads to reduce the transition probabilities and lead to hypochromism (Abdel-Rahman et al., 2016 a,b,c). The range of the hypochromism or hyperchromism in the charge transfer from metal-to-ligand (MLCT) band is commonly consistent with the force of intercalation interaction (Biancardi et al., 2014; Abdel-Rahman et al., 2015a,b; Abu-Dief et al., 2016). The electronic absorption spectra of ESPNMn complex in the absence and presence of various concentrations of molar solution CT-DNA are shown in Figures 6, S4. extension of rising quantity of molar solution CT-DNA leads to a reduction of absorbance for a metal chelate. The spectral parameters and b for the DNA interaction with the tested metal chelates are shown in Table S6. The tested metal chelates could bind to DNA mainly through an intercalative and replacement modes through the series: ESPNMn > ESPNV complex (Abdel-Rahman et al., 2016a–d; 2017a,b).

#### 3.3.2. Viscosity measurements

Hydrodynamic methods are sensible to length increment or reduce of DNA are considered as the most efficient methods of studying the binding mode of compounds to DNA. Under suitable conditions, a traditional intercalative mode such as intercalation of drugs such as ethidium bromide leads to a significant increment in the viscosity of DNA solution because of an increment in the segregation of base pairs at the intercalation site and hence an increment in the inclusive DNA length. On other hand, drug molecules

attachment obviously to the DNA grooves lead to less pronounced in DNA solution viscosity (Raja et al., 2012) a partial intercalation of complexes could bend the DNA helix, producing in the reduction of its efficient length and, concomitantly, its viscosity (Liu et al., 2008). The relative viscosity of DNA solution promotes significantly as the quantity of the compound raises, as indicated in Fig. 7. This might be because of the admission of the aromatic ring in imine ligand into the DNA base pairs which result in a crook in the DNA helix, hence, increase in the segregation of the base pairs at the intercalation place and increment in DNA molecular length.

#### 3.3.3. Gel electrophoresis

The gel electrophoresis image clearly showed that the intensity of all the processed DNA samples has partially detracted, probably due to the interaction with DNA (cf. Fig. 8). The fractional binding of DNA was spotted in the prepared imine chelates. The various was clarified in the bands of the prepared metal chelates contrasted with that of the observation DNA. This explains that the observation DNA alone does not indicate any visible cleavage whereas the metal chelates suggest cleavage (Mishra, 2012). As the compound was observed to bind with DNA, it can be concluded that the compound reduces the growth of the pathogenic organism by interaction with genome. The tested results suggested that the checked chelates can bind to DNA through intercalative mode.

### 3.4. Anticancer activity

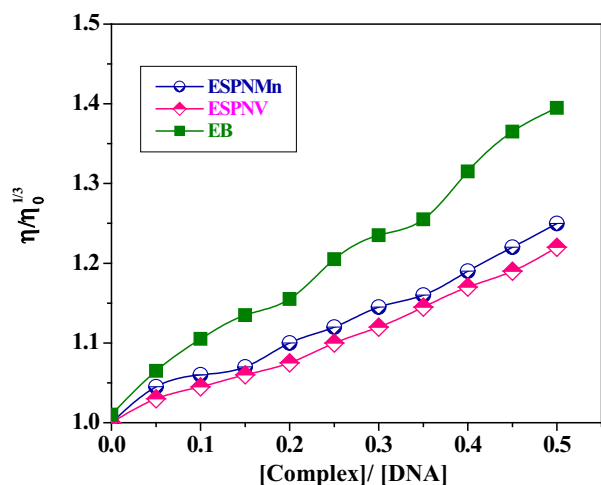
The cytotoxic potency of ESPN imine ligand and its chelates was evaluated and results are shown in Fig. 9 and Table S7. As offered, the prepared complexes showed manifestly cytotoxic potencies (which are higher than that of ligand) assisted to vinblastine standard drug. It appears that variation in the complexation locations and the quality of the metal ion have influence on the biological way. ESPNV complex shows higher cytotoxicity effect than ESPNMn complex in case of all the tested cancer cells. The refinement of cytotoxic potency might be specified to that the positive charge of the metal increased the acidity of arranged ligand that gives protons, which cause more potent hydrogen bonds which promoted the biological activity (Feng et al., 2006). It appears that variation the complexation locations and the quality of the metal ion has an obvious impact on the biological way through modifying the binding strength of DNA (Abdel-Rahman et al., 2016c; 2017b).

## 4. Conclusions

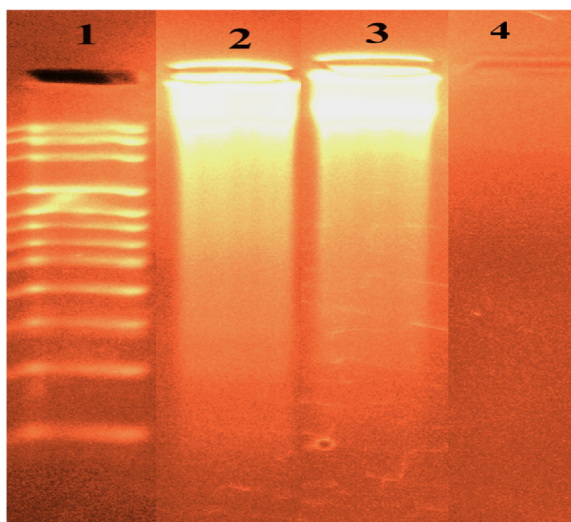
In this study VO(II) and Mn(II) imine chelates have been synthesized and their structures have been characterized. The obtained results demonstrated that the ESPN imine ligand behaves as dibasic tetra-dentate ONNO ligand and coordinates to VO(II) and Mn(II) in 1:1 M ratio. From the spectral and analytical data, it is observed that the metal chelates adopted octahedral geometry in case of Mn(II) and square pyramidal geometry in VO(II). The anti-pathogenic screening showed that these complexes are perfect antimicrobial agents against different organisms. Moreover, DNA interaction studies propose the intercalative and replacement modes of interaction. Furthermore, the growth inhibitory effect of the prepared

Table 3  
Minimum inhibition concentration (MIC) for antimicrobial assay of the investigated compounds.

Compounds	Bacteria.			Fungi		
	<i>E. coli</i>	<i>B. subtilis</i>	<i>S. aureus</i>	<i>A. flavus</i>	<i>C. albicans</i>	<i>T. rubrum</i>
ESPN	6	5.5	5	6	5	5.5
ESPMn	4	5	3	1	2.5	2
ESPNV	2.5	3	2	0.5	2	1



**Fig. 7.** The impact of increasing concentration of the prepared metal chelates on the proportional viscosities of DNA at [DNA] = 0.5 mM, [complex] and [EB] = 25–250 μM and 298 K.



**Fig. 8.** DNA binding results of the tested imine metal chelates based on gel electrophoresis. Lane 1: DNA Ladder, lane 2: ESPNV + DNA, lane 3: ESPMn + DNA, lane 4: ESPNV complex.

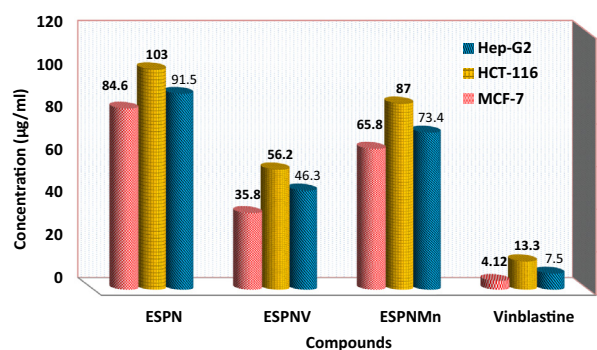


**Fig. 9.** IC<sub>50</sub> values of ESPN imine ligand and its complexes against HCT-116 cell line, HepG-2 cell line, and MCF-7 cell line.

compounds was tested on HepG-2, HCT-116 and MCF-7 cancer cells. These biological returns from our investigation would be helpful in conscious of DNA interaction exposed by metal chelates

and could progress to improve novel metal based therapeutic drugs.

## Appendix A. Supplementary data

Supplementary data associated with this article can be found, in the online version, at <http://dx.doi.org/10.1016/j.jksus.2017.05.011>.

## References

- Abu-Dief, A.M., Mohamed, I.M.A., 2015. *J. Basic Appl. Sci.* 4, 119–133.
- Abu-Dief, A.M., Mohammed, S.M.A., García-Granda, S., 2015. *Acta Cryst. E* 71, 496–497.
- Abdel Rahman, L.H., Abu-Dief, A.M., Moustafa, H., Hamdan, S.K., 2017a. Ni(II) and Cu(II) complexes with ONNO asymmetric tetradentate Schiff base ligand: synthesis, spectroscopic characterization, theoretical calculations, DNA interaction and antimicrobial studies. *Appl. Organometal. Chem.* 31, e3555.
- Abdel-Rahman, L.H., Ismail, N.M., Ismael Mohamed, Abu-Dief, A.M., Ahmed, E.A., 2017b. Synthesis, characterization, DFT calculations and biological studies of Mn(II), Fe(II), Co(II) and Cd(II) complexes based on a tetradentate ONNO donor Schiff base ligand. *J. Mol. Struct.* 1134, 851–862.
- Abdel-Rahman, L.H., Abu-Dief, A.M., Aboelez, M.O., Abdel-Mawgoud, A.A.H., 2017c. *J. Photochem. Photobiol. B* 170, 271–285.
- Abdel-Rahman, L.H., Abu-Dief, A.M., Basha, M., Abdel-Mawgoud, A.A.H., 2017d. e3750. <https://doi.org/10.1002/aoc.3750>.
- Abdel-Rahman, L.H., Ismail, N.M., Ismael, M., Abu-Dief, A.M., 2017e. *Inorg. and Nano-Metal Chem.* 47, 467–480.
- Abdel-Rahman, L.H., El-Khatib, R.M., Nassr, L.A.E., Abu-Dief, A.M., Lashin, F.E., 2013. Design, characterization, teratogenicity testing, antibacterial, antifungal and DNA interaction of few high spin Fe(II) Schiff base amino acid complexes. *Spectrochim. Acta Part A* 111, 266–276.
- Abdel-Rahman, L.H., El-Khatib, R.M., Nassr, L.A.E., Abu-Dief, A.M., Lashin, F.E., Ismael, M., 2014. Metal based pharmacologically active agents: Synthesis, structural characterization, molecular modeling, CT-DNA binding studies and in vitro antimicrobial screening of iron(II) bromosalicylidene amino acid chelates. *J. Spectrochim. Acta Part A* 117, 366–378.
- Abdel-Rahman, L.H., Abu-Dief, A.M., Hamdan, S.K., Seleem, A.A., 2015a. *Int. J. Nano. Chem.* 1, 65–77.
- Abdel Rahman, L.H., Abu-Dief, A.M., Hashem, N.A., Seleem, A.A., 2015b. Recent advances in synthesis, characterization and biological activity of nano sized schiff base amino acid M(II) complexes. *Int. J. Nano. Chem.* 1, 79–95.
- Abdel-Rahman, L.H., Abu-Dief, A.M., El-Khatib, R.M., Abdel-Fatah, S.M., 2016a. A). Sonochemical synthesis, DNA binding, antimicrobial evaluation and in vitro anticancer activity of three new nano-sized Cu(II), Co(II) and Ni(II) chelates based on tri-dentate NOO imine ligands as precursors for metal oxides. *J. Photochem. Photobiol. B* 162, 298–308.
- Abdel-Rahman, L.H., Abu-Dief, A.M., Ismael, M., Mohamed, M.A.A., Hashem, N.A., 2016b. B). Synthesis, structure elucidation, biological screening, molecular modeling and DNA binding of some Cu(II) chelates incorporating imines derived from amino acids. *J. Mol. Struct.* 1103, 232–244.
- Abdel-Rahman, L. H., Abu-Dief, A. M.; Newair, E. F., Hamdan, S. K. (2016 c). Some new nano-sized Cr(III), Fe(II), Co(II), and Ni(II) complexes incorporating 2-((E)-(pyridine-2-ylimino)methyl)naphthalen-1-ol ligand: Structural characterization, electrochemical, antioxidant, antimicrobial, antiviral assessment and DNA interaction *J. Photochem. Photobiol. B* 160, 18–31.
- Abdel-Rahman, L.H., Abu-Dief, A.M., Adam, M.S.S., Hamdan, S.K., 2016d. Some new nano-sized mononuclear Cu(II) Schiff base complexes: design, characterization, molecular modeling and catalytic potentials in benzyl alcohol oxidation. *Catal. Lett.* 146, 1373–1396.
- Abu-Dief, A.M., Nassr, L.A.E., 2015. Tailoring, physicochemical characterization, antibacterial and DNA binding mode studies of Cu(II) Schiff bases amino acid bioactive agents incorporating 5-bromo-2-hydroxybenzaldehyde. *J. Iran. Chem. Soc.* 12, 943–955.
- Abu-Dief, A.M., Díaz-Torres, R.E., Sañudo, C., Abdel-Rahman, L.H., Alcalde, N.A., 2013. Novel sandwich triple-decker dinuclear Nd(III)-(bis-N, N0-p-bromosalicylideneamino-1,2-diaminobenzene) complex. *Polyhedron* 64, 203–208.
- Abu-Dief, A.M., Nassar, I.F., Elsayed, W.H., 2016. Magnetic NiFe<sub>2</sub>O<sub>4</sub> nanoparticles: efficient, heterogeneous and reusable catalyst for synthesis of acetylferrocene chalcones and their anti-tumour activity. *Appl. Organometal. Chem.* 30, 917–923.
- Alaghaz, A.N.M.A., Zayed, M.E., Alharbi, S.A., Ammar, R.A.A., 2015. *J. Mol. Struct.* 1087, 60–67.
- Al-Mogren, M.M., Alaghaz, A.M.A., Ebrahim, E.A., 2013. *Spectrochim. Acta A* 114, 695–707.
- Begum, M.S.A., Saha, S., Nethaji, M., Chakravarty, A.R., 2010. *J. Inorg. Biol. Chem.* 104, 477–484.
- Biancardi, A., Burgalassi, A., Terenzi, A., Spinello, A., Barone, G., Biver, T., Mennucci, B., 2014. *Chem. A Eur. J.* 20, 7439–7447.
- Canali, L., Sherrington, D.C., 1999. Utilisation of homogeneous and supported chiral metal(salen) complexes in asymmetric catalysis. *Chem. Soc. Rev.* 28, 85–93.



- Canpolat, E., Kaya, M., 2002. *J. Coord. Chem.* 55, 961–968.
- Chandra, S., Raizada, S., Tyagi, M., Sharma, P., 2008. *Spectrochim. Acta A* 69, 816.
- Datta, A., Karan, N.K., Mitra, S., Rosair, G., 2002. *Z. Naturforsch* 57b, 999–1002.
- Dyer, J.R., 1965. *Applications of Absorption Spectroscopy of Organic Compounds*. Prentice-Hall, Englewood Cliffs, NJ, USA.
- El-Shiekh, R., Akl, M., Gouda, A., Ali, W., 2011. *J. Am. Sci.* 7 (4), 797–807.
- El-Tabl, A.S., EL-Saied, F.A., Al-Hakimi, A.N., 2008. *J. Coord. Chem.* 61 (15), 2380–2401.
- Feng, G., Mareque-Rivas, J.C., Williams, N.H., 2006. *Chem. Comm.* 17, 1845–1847.
- Gupta, K.C., Sutar, A.K., 2007. Polymer anchored Schiff base complexes of transition metal ions and their catalytic activities in oxidation of phenol. *J. Mol. Catal. A: Chem.* 272, 64–74.
- Gupta, K.C., Sutar, A.K., Lin, C.C., 2009. Polymer supported Schiff base complexes in oxidation reactions. *Coord. Chem. Rev.* 253, 1926–1946.
- Hindo, S.S., Frezza, M., Tomco, D., Heeg, M.J., Hryhorczuk, L., McGarvey, B.R., Dou, Q. P., Verani, C.N., 2009. *Eur. J. Med. Chem.* 44, 4353–4361.
- Keypour, H., Rezaeivala, M., Valencia, L., Pérez-Lourido, P., 2008. *Polyhedron* 27 (16), 3172–3176.
- Lacroix, J., 2001. Second-order optical nonlinearities in coordination chemistry: the case of bis(salicylaldiminato)metal Schiff base complexes. *Eur. J. Inorg. Chem.* 2, 339–348.
- Ligtenberg, A.G.J., Hage, R., Feringa, B.L., 2003. *Coord. Chem. Rev.* 237, 89–101.
- Lin, X., Doble, D.M.J., Blake, A.J., Harrison, C., Wilson, C., Schrder, M., 2003. *J. Am. Chem. Soc.* 125, 9476–9483.
- Liu, Y., Mei, W., Lu, J., Zhao, H., He, L., Wu, F., 2008. *J. Coord. Chem.* 61, 3213–3224.
- Majumder, S., Hazra, S., Dutta, S., Biswas, P., Mohanta, S., 2009. Syntheses, structures and electrochemistry of manganese(III) complexes derived from N, N0-o-phenylenebis(3-ethoxysalicylaldimine): Efficient catalyst for styrene epoxidation. *Polyhedron* 28, 2473–2479.
- Maneiro, M., Bermejo, M.R., Fondo, M., Gonzalez, A.M., Rey, M., Sanmart, J.S., 2001. Electrochemical synthesis of manganese(II)-Schiff base complexes and their behaviour towards H<sub>2</sub>O, H<sub>2</sub>O<sub>2</sub> and SO<sub>2</sub>. *Transition Metal Chem.* 26, 120–126.
- Mounika, K., Anupama, B., Pragathi, J., Gyanakumari, C., 2011. Synthesis, characterization and biological activity of a schiff base derived from 3-ethoxy salicylaldehyde and 2-amino benzoic acid and its transition metal complexes. *J. Sci. Res.* 2 (3), 513–524.
- Nejo, A.A., Kolawole, G.A., Nejo, A.O., Segapelo, T.V., Muller, C.J., 2011. Synthesis, structural, and insulin-enhancing studies of oxovanadium(IV) complexes. *Aust. J. Chem.* 64, 1574–1579.
- Raja, D., Bhuvanesh, S.S.P., Natarajan, K., 2012. *Jo. Biolog. Inorg. Chem.* 17, 223–237.
- Raman, N., Kulandaisamy, A., Jeyasubramanian, K., 2002. Synthesis, spectral, redox and biological studies of some Schiff base copper(II), nickel(II), cobalt(II), manganese(II), zinc(II) and oxovanadium(II) complexes derived from 1-phenyl-2,3-dimethyl-4-(4-iminopentan-2-one)-pyrazol-5-one and 2-aminophenol/2-aminothiophenol. *Indian J. Chem.* 41A, 942–949.
- Rapheal, P.F., Manoj, E., Kurup, P.R., 2007. *Polyhedron* 26, 818.
- Rayati, S., Ghaemi, A., Sadeghzadeh, N., 2010. *Catal. Commun.* 11, 792–796.
- Shakir, M., Sherwani, M.A., Mohammad, O., Azam, M., Al-Resayes, S., 2016. *J. Photochem. Photobiol. B.* 157, 39–56.
- Silverstein R.M., Webster, F.X., 1997. Sixth ed. John Wiley & Sons, New York, NY, USA.
- Tisato, J., Refosco, F., Bandoli, F., 1994. Structural survey of technetium complexes. *Coord. Chem. Rev.* 135, 325–397.
- Yousef, T.A., Abu El-Reash, G.M., Gabr, I.M., El-Gammal, O.A., Bedier, R.A., 2012. Structural survey of technetium complexes. *J. Mol. Struct.* 1029, 149.